Egypt.J.Chem. **Vol. 63**, No. 6. pp. 2157 - 2176 (2020)

Egyptian Journal of Chemistry
http://ejchem.journals.ekb.eg/

Nano Schiff Base and Its Metal Complexes: Synthesis, Characterization Tools, Biological Applications and Molecular Docking Studies

Walaa H. Mahmoud[1,2]*, Ahmed M. Refaat[1], Gehad G. Mohamed[1,2]
[1] *Chemistry Department, Faculty of Science, Cairo University, Giza, 126103, Egypt*
[2] *Egypt Nanotechnology Center, Cairo University, El-Sheikh Zayed, 6th October, Giza, 12588, Egypt.*

A TOTAL of eight new metal complex derivatives of 4,4'-((1Z,1'Z)-(naphthalene-1,8-diylbis(azanylylidene))bis(methanylylidene))dibenzaldehyde, H_2L with the metal ions Cr(III), Mn(II), Fe(III), Co(II), Ni(II), Cu(II), Zn(II) and Cd(II) have been successfully prepared in alcoholic medium. The complexes obtained are characterized quantitatively and qualitatively by using micro elemental analysis, conductivity measurements, FT-IR spectroscopy, UV–Vis spectroscopy, mass spectroscopy, ^{1}HNMR, magnetic susceptibility, thermal (TG/DTG) and SEM data to illuminate their structures. The data showed that the complexes had composition of MH_2L type. From the spectral study, all the complexes obtained as monomeric structure and the metals center moieties are six-coordinated with an octahedral geometry. ^{1}H NMR spectral data of the ligand (H_2L) and its Zn(II) and Cd(II) complexes agreed well with the proposed structures. Thermogravimetric data (TG and DTG) were also studied. SEM analysis confirm the nano-structures of the ligand and some of its complexes. The preliminary in vitro antibacterial and antifungal screening activity revealed that complexes showed moderate activity against tested bacterial strains and slightly higher compared to the ligand (H_2L). Anticancer activity of the ligand and its metal complexes were evaluated in human cancer (MCF-7 cells viability). The IC_{50} of the cadmium complex is 17.6 mg/mL, which revealed its high activity. The binding between H_2L with receptors of crystal structure of *S. aureus* (PDB ID: 3Q8U), crystal structure of sialidase NanC of *Streptococcus pneumoniae* (4YW4), receptors of breast cancer mutant oxidoreductase (PDB ID: 3HB5) and crystal structure of *Escherichia coli* (PDB ID: 3T88) were expected and set in details using molecular docking. The data showed that the most effective binding energy with 3Q8U receptor which is -11.3 kcal/mol.

Keywords: Schiff base; 1,8-diaminonaphthalene; TG/DTG; Nano structure; Antibacterial; Anticancer activity.

Introduction

Synthesis and characterization of new coordination compounds have always been a challenge to the inorganic chemists since they were identified in the nineteenth century. Transition metal complexes of symmetrical and asymmetrical Schiff bases have played a significant role in the field of coordination, inorganic and bioinorganic chemistry as models for biological, analytical and industrial applications. The work herein deals with the synthesis, characterization and in vitro biological studies of metal complexes of the synthesized Schiff base.

Schiff bases are condensation products of primary amines with carbonyl compounds and they were first reported by Schiff [1] in 1864. The common structural feature of these compounds is the azomethine group with a general formula RHC=N-R1, where R and R1 are alkyl, aryl, cyclo alkyl or heterocyclic groups which may be variously substituted. These compounds are also known as anils, imines or azomethines. Several studies [2-8] showed that the presence of a lone pair of electrons in a sp^2 hybridized orbital of nitrogen atom of the azomethine group is of considerable chemical and biological importance.

Corresponding author:dr.walaa@yahoo.com; wmahmoud@sci.cu.edu.eg
Received 12/10/2019; Accepted 3/12/2019
DOI: 10.21608/ejchem.2019.18109.2104

Because of the relative easiness of preparation, synthetic flexibility, and the special property of C=N group, Schiff bases are generally excellent chelating agents[6-12] especially when a functional group like –OH or –SH is present close to the azomethine group so as to form a five or six membered ring with the metal ion. Versatility of Schiff base ligands and biological, analytical and industrial applications of their complexes make further investigations in this area highly desirable.

Nowadays, the research field dealing with Schiff base coordination chemistry had expanded enormously. The importance of Schiff base complexes for bioinorganic chemistry, biomedical applications, supramolecular chemistry, catalysis and material science, separation and encapsulation processes, and formation of compounds with unusual properties and structures has been well recognized and reviewed. Synthetic method for the preparation of pyrimidines is the condensation reaction of 1,8-diaminonaphthalene (1,8-DAN) with various carbonyl groups, which requires a special reagent or force reaction conditions. Usually, the product of this condensation is Schiff base, however when 1,8-DAN is used as primer diamine it can be obtained pyrimidine or its derivatives [8, 12]

So, the aim of this work is to synthesize and characterize Schiff base (H_2L) ligand (see Scheme. 1) and its ligand chelates with eight transition metal ions: Cr(III), Mn(II), Fe(III), Co(II), Ni(II), Cu(II), Zn(II) and Cd(II), in order to study the effect of the chelation process on the physicochemical properties and biological applications.

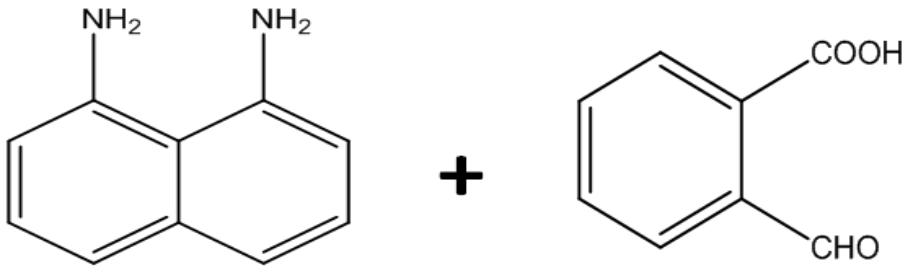

Reflux about 2h

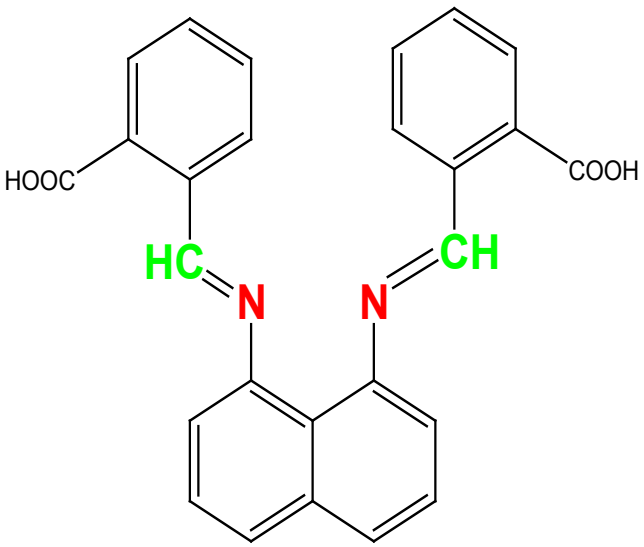

2,2'-((1*E*,1'*E*)-(naphthalene-1,8-diylbis(azanylylidene))bis(methanylylidene))dibenzoic acid

Scheme. 1. Preparation of H2L Schiff base ligand.

Experimental

Materials and reagents

All chemicals used were of the analytical reagent grade (AR) and of highest purity available. The chemicals used included 1,8-diaminonaphthalene (Sigma-Aldrich), Phthalaldehydic acid (Merck, Germany), $CrCl_3.6H_2O$, $MnCl_2.2H_2O$ and $FeCl_3.6H_2O$ (Sigma-Aldrich, Germany), $NiCl_2.6H_2O$, $CoCl_2.6H_2O$, $CuCl_2.2H_2O$ and $ZnCl_2$ (BDH) and $CdCl_2$ (Merck, Germany). Organic solvents used were ethyl alcohol (95 %), methyl alcohol and N,N-dimethylformamide (DMF). Deionized water was usually used in all preparations. Human tumor cell line (Breast cell) was obtained frozen in liquid nitrogen (-180 °C) from the American Type Culture Collection. The tumor cell line (MCF7) was maintained in the National Cancer Institute, Cairo, Egypt, by serial subculturing.

Solutions

Stock solutions of the Schiff base ligand and its metal complexes of $1X10^{-3}$ M were prepared by dissolving an accurately weighed amount in N,N-dimethylformamide. The conductivity then measured for the metal complexes solutions. Dilute solutions of the Schiff base ligand and its metal complexes ($1 X 10^{-4}$ M) were prepared by accurate dilution from the previous prepared stock solutions for measuring their UV–Vis spectra.

Solution of anticancer study

A fresh stock solution (1×10^{-3} M) of Schiff base ligand ($0.12 X 10^{-2}$ g l^{-1}) was prepared in the appropriate volume of DMF. DMSO was used in cryopreservation of cells. RPMI-1640 medium was used. The medium was used for culturing and maintenance of the human tumor cell line. The medium was supplied in a powder form. It was prepared as follows: 10.4 g of medium was weighed, mixed with 2 g of sodium bicarbonate, completed to 1 L with distilled water and shaken carefully until complete dissolution. The medium was then sterilized by filtration in a Millipore bacterial filter (0.22 ml). The prepared medium was kept in a refrigerator (4 °C) and checked at regular intervals for contamination. Before use, the medium was warmed at 37 °C in a water bath and supplemented with penicillin–streptomycin and FBS. Sodium bicarbonate was used for the preparation of RPMI-1640 medium. Isotonic trypan blue solution (0.05%) was prepared in normal saline and was used for viability counting. FBS (10%, heat inactivated at 56 °C for 30 min), 100 units/mL penicillin and 2 mg/ml streptomycin were used for the supplementation of RPMI-1640 medium prior to use. Trypsin ($0.25 X 10^{-1}$% w/v) was used for the harvesting of cells. Acetic acid (1% v/v) was used for dissolving unbound SRB dye. SRB (0.40%) dissolved in 1% acetic acid was used as a protein dye. A stock solution of trichloroacetic acid (50%) was prepared and stored. An amount of 50 µL of the stock was added to 200 µL of RPMI-1640 medium per well to yield a final concentration of 10% used for protein precipitation. Isopropanol (100%) and ethanol (70%) were used. Tris base (10 mM; pH = 10.50) was used for SRB dye solubilization. Tris base (121.10 g) was dissolved in 1000 ml of distilled water and the pH was adjusted using hydrochloric acid (2 M).

Instrumentation

Microanalyses of carbon, hydrogen and nitrogen were carried out at the Microanalytical Center, Cairo University, Egypt, using a CHNS-932 (LECO) Vario elemental analyzer. Analyses of the metals were conducted by dissolving the solid complexes in concentrated HNO_3, and dissolving the residue in deionized water. The metal content was carried out using inductively coupled plasma atomic absorption spectrometry (ICP-AES), Egyptian Petroleum Research Institute. Fourier transform infrared (FT-IR) spectra were recorded with a Perkin Elmer 1650 spectrometer (400-4000 cm^{-1}) in KBr pellets. ^{1}H-NMR spectra, as solutions in DMSO-d^6, were recorded with a 300 MHz Varian-Oxford Mercury at room temperature using tetra-methylsilane as an internal standard. Mass spectra were recorded using the electron ionization technique at 70 eV with an MS-5988 GS-MS Hewlett-Packard instrument at the Microanalytical Center, National Center for Research, Egypt. UV–visible spectra were obtained with a Shimadzu UVmini-1240 spectrophotometer. Molar conductivities of 10^{-3} M solutions of the solid complexes in DMF were measured using a Jenway 4010 conductivity meter. Thermogravimetric (TG) and differential thermogravimetric (DTG) analyses of the solid complexes were carried out from room temperature to 1000 °C using a Shimadzu TG-50H thermal analyzer. The scanning electron microscope (SEM) image of the complexes was recorded by using SEM Model Quanta 250 FEG (Field Emission Gun) attached with EDX unit (Energy Dispersive X-ray Analyses), with accelerating voltage 30 K.V., magnification

14X up to 1000000 and resolution for Gun.1n, National Research Center, Egypt. Antimicrobial measurements were carried out at the Microanalytical Center, Cairo University, Egypt. Anticancer activity experiments were performed at the National Cancer Institute, Cancer Biology Department, Pharmacology Department, Cairo University. The optical density (OD) of each well was measured spectrophotometrically at 564 nm Cancer Biology Department, Pharmacology Department, Cairo University. The optical density (OD) of each well was measured spectrophotometrically at 564 nm with an ELIZA microplate reader (Meter tech. R960, USA).

Synthesis of Schiff base ligand (H_2L)

The Schiff base ligand (H_2L) was prepared by refluxing a mixture of 1,8-diaminonaphthalene (0.025 mol, 4.00 g) dissolved in ethanol and phthalaldehydic acid (0.025 mol, 7.60 g) dissolved in methanol. The resulting mixture was stirred under reflux for about 2 hours, during which a dark brown solid compound was separated. It was filtered, recrystallized using acetonitrile, washed with diethylether and dried in vacuum. Yield 91%; m.p. 161 °C; brown solid. Anal. Calcd for $C_{26}H_{18}N_2O_4$ (%): C, 73.93; H, 4.26; N, 6.63; Found (%): C, 73.12; H, 3.98; N, 6.11. FT-IR (cm^{-1}): azomethine ν(C=N) 1610sh, ν(OH) 3429 br, $\nu(COO)_{asym}$ 1593sh and $\nu(COO)_{sym}$ 1432sh. ^1H NMR (300 MHz, DMSO-d_6, δ, ppm): 10.11 (s, 2H, carboxylic proton), 8.08 (m, 2H, CH proton), 7.00-7.55 (m, 14H, aromatic ring). λ_{max} (nm): 280 (π –π*), 340 (n –π*) and ٤42 (charge transfer).

Synthesis of metal complexes

The Cr(III), Mn(II), Fe(III), Co(II), Ni(II), Cu(II), Zn(II) and Cd(II) complexes were prepared by a reaction of 1:1 molar mixture of hot ethanolic solution (60 °C) of the metal chloride (1.10 X 10^{-3} mol) and the DMF solution of Schiff base ligand (H_2L) (0.40 g, 1.10 X 10^{-3} mol). The resulting mixture was stirred under refluxing for one hour, during which the complexes were precipitated. They were collected by filtration and purified by washing several times with diethyl ether. The solid complexes then dried in desiccator over anhydrous calcium chloride. The percent yield was ranged from 81 to 92%.

$[Cr(H_2L)(H_2O)_3Cl]Cl_2.2H_2O$

Yield 89%; m.p. >300 °C; brown. Anal. Calcd for $C_{26}H_{28}Cl_3CrN_2O_9$ (%): C, 46.56; H, 4.17; N, 4.18; Cr, 7.76; Found (%): C, 46.08; H, 3.86; N, 4.04; Cr, 7.16. FT-IR (ν, cm^{-1}): ν(OH) 3416br, azomethine (C=N) 1622sh, ν(COO)asym 1593sh, ν(COO)sym 1432sh, H_2O stretching of coordinated water 900w and 890s, (M─O coordinated water) 513m, (M─N) 480w. UV-vis (λ_{max}, nm): 330 (n–π*).

$[Mn(H_2L)(H_2O)_3Cl]Cl.H_2O$

Yield 88%; m.p. 300 °C; Reddish brown. Anal. Calcd for $C_{26}H_{26}Cl_2MnN_2O_8$ (%): C, 41.93; H, 4.19; N, 4.51; Mn, 8.87; Found (%): C, 41.23; H, 3.77; N, 3.89; Mn, 8.11. FT-IR (ν, cm^{-1}): ν(OH) 3432br, azomethine (C=N) 1630sh, ν(COO)asym 1595sh, ν(COO)sym 1433sh, H_2O stretching of coordinated water 923w and 820s, (M─O coordinated water) 549 m, (M─N) 481w. UV-vis (λ_{max}, nm): 340 (n–π*).

$[Fe(H_2L)(H_2O)_3Cl]Cl_2.2H_2O$

Yield 92%; m.p. >300 °C; Reddish yellow. Anal. Calcd for $C_{26}H_{28}Cl_3FeN_2O_9$ (%): C, 46.26; H, 4.15; N, 4.15; Fe, 8.31; Found (%): C, 45.87; H, 3.79; N, 3.80; Fe, 7.87. FT-IR (ν, cm^{-1}): ν(OH) 3431br, azomethine (C=N) 1625sh, ν(COO)asym 1589sh, ν(COO)sym 1435sh, H_2O stretching of coordinated water 909w and 823s, (M─O coordinated water) 543 w, (M─N) 475w. UV-vis (λ_{max}, nm): 281 (π–π*).

$[Co(H_2L)(H_2O)_3Cl]Cl.H_2O$

Yield 88%; m.p. 290 °C; Brown solid. Anal. Calcd for $C_{26}H_{26}Cl_2CoN_2O_8$ (%): C, 50.05; H, 4.16; N, 4.48; Co, 9.45; Found (%): C, 49.55; H, 3.76; N, 4.03; Co, 8.97. FT-IR (ν, cm^{-1}): ν (OH) 3425br, azomethine (C=N) 1635sh, ν(COO)asym 1590sh, ν(COO)sym 1439sh, H_2O stretching of coordinated water 920w and 823s, (M─O coordinated water) 539w, (M─N) 461w. UV-vis (λ_{max}, nm): 282 (π–π*).

2.6.5 $[Ni(H_2L)(H_2O)_3Cl]Cl.H_2O$

Yield 81%; m.p. 290 °C; Brown solid. Anal. Calcd for $C_{26}H_{26}Cl_2NiN_2O_8$ (%): C, 50.04; H, 4.16; N, 4.49; Ni, 9.43; Found (%): C, 49.67; H, 3.88; N, 4.91; Ni, 9.91. FT-IR (ν, cm^{-1}): ν(OH) 3427br, azomethine (C=N) 1627sh, ν(COO)asym 1591sh, ν(COO)sym 1439sh, H_2O stretching of coordinated water 962w and 820w, (M─O coordinated water) 536w, (M─N) 481w. UV-vis (λ_{max}, nm): 338(n–π*).

$[Cu(H_2L)(H_2O)_3Cl]Cl.H_2O$

Yield 82%; m.p. 280 °C; dark brown solid. Anal. Calcd for $C_{26}H_{26}Cl_2CuN_2O_8$ (%): C, 41.40; H, 4.14; N, 4.45; Cu, 10.11; Found (%): C, 40.22; H, 4.09; N, 4.34; Cu, 10.03 FT-IR (ν, cm^{-1}): ν(OH) 3433br, azomethine (C=N) 1625sh, ν(COO)asym

1590sh, ν(COO)sym 1440sh, H_2O stretching of coordinated water 915w and 829w, (M─O coordinated water) 539w, (M─N) 472w. UV-vis (λ_{max}, nm): 279(π–π*).

[Zn(H$_2$L)(H$_2$O)$_2$Cl$_2$]2H$_2$O

Yield 85%; m.p. >300 °C; Reddish brown solid. Anal. Calcd for $C_{26}H_{26}Cl_2ZnN_2O_8$ (%): C, 49.52; H, 4.12; N, 4.44; Zn, 10.31; Found (%): C, 49.32; H, 4.03; N, 4.13; Zn, 10.24. FT-IR (ν, cm^{-1}): ν(OH)3436br, azomethine (C=N) 1635sh, ν(COO)asym 1592sh, ν(COO)sym 1436sh, H_2O stretching of coordinated water 907w and 825w, (M─O coordinated water) 536 w, (M─N) 482w. ^{1}H NMR (300 MHz, DMSO-d$_6$, δ, ppm): 10.01 (s, 2H, carboxylic group), 8.13 (m, 2H, CH group), 7.10-7.50 (m, 14H, aromatic ring). UV-vis (λ_{max}, nm): 282(π–π*).

[Cd(H$_2$L)(H$_2$O)$_2$Cl$_2$]2H$_2$O

Yield 90%; m.p. >300 °C; Reddish brown solid. Anal. Calcd for $C_{26}H_{26}Cl_2CdN_2O_8$ (%): C, 46.01; H, 3.83; N, 4.12; Cd, 16.66; Found (%): C, 45.91; H, 3.72; N, 4.03; Cd, 16.34. FT-IR (ν, cm^{-1}): ν(OH) 3433br, azomethine (C=N) 1619sh, ν(COO)asym 1590sh, ν(COO)sym 1439sh, H_2O stretching of coordinated water 923w and 834w, (M─O coordinated water) 532w, (M─N) 457w. ^{1}H NMR (300 MHz, DMSO-d$_6$, δ, ppm): 10.01 (s, 2H, carboxylic group), 7.12-7.43 (m, 14H, aromatic ring).

Spectrophotometric studies

The absorption spectra were recorded for 1 X 10^{-4} M solutions of the free Schiff base ligand and its metal complexes that dissolved in DMF. The spectra were scanned within the wavelength range from 200 to 700 nm.

Antimicrobial activity

The tests for in vitro antibacterial and antifungal activities were performed through the disc diffusion method [13]. The bacterial organisms used were Gram (+) bacteria: [*Streptococcus pneumoniae*, *Bacillus Subtilis*], Gram(−) bacteria: [*Escherichia coli, Pseudomonas aeruginosa*] and fungal specie include [*Candida albicans*, and *Aspergillus albicans*]. Stock solution (0.001 mol) was prepared by dissolving the compounds in DMSO. The nutrient agar medium for antibacterial was (0.50% Peptone, 0.10% Beef extract, 0.20% Yeast extract, 0.50% NaCl and 1.50% Agar-Agar) was prepared, cooled to 47 °C and seeded with tested microorganisms. After solidification 5 mm diameter holes were punched by a sterile corkborer. The investigated compounds, i.e. Schiff base ligand and their metal complexes, were introduced in Petri-dishes (only 0.1 m) after dissolving in DMSO at 1.0 x 10^{-3} M. These culture plates were then incubated at 37 °C for 20 h for bacteria. The activity was determined by measuring the diameter of the inhibition zone (in mm). The plates were kept for incubation at 37 °C for 24 h and then the plates were examined for the formation of zone of inhibition. The diameter of the inhibition zone was measured in millimeters. Antimicrobial activities were performed in triplicate and the average was taken as the final reading [14].

Anticancer activity

Potential cytotoxicity of the compounds was tested using the method of Skehan and Storeng [15]. Cells were plated in 96-multiwell plate (104 cells/well) for 24 h before treatment with the compounds to allow attachment of cell to the wall of the plate. Different concentrations of the compounds under investigation (0, 5, 12.5, 25, 50 and 100 µg/ ml) were added to the cell monolayer and triplicate wells were prepared for each individual dose. The monolayer cells were incubated with the compounds for 48 h at 37 °C and in 5% CO_2 atmosphere. After 48 h, cells were fixed, washed and stained with SRB stain. Excess stain was washed with acetic acid and attached stain was recovered with tris-EDTA buffer. The optical density (O.D.) of each well was measured spectrophotometrically at 564 nm with an ELIZA microplate reader, the mean background absorbance was automatically subtracted and mean values of each drug concentration was calculated. The relation between drug concentration and surviving fraction is plotted to get the survival curve of breast tumor cell line for each compound.

Calculation

The percentage of cell survival was calculated as follows:

Survival fraction = O.D. (treated cells) / O.D.(control cells).

The IC50 values (the concentrations of the Schiff base ligand (L) or its metal complexes required to produce 50% inhibition of cell growth). The experiment was repeated 3 times.

Molecular docking

Crystal structure of *S. aureus* (PDB ID: 3Q8U), crystal structure of sialidase NanC of *Streptococcus pneumoniae* (PDB ID:

4YW4), receptors of breast cancer mutant oxidoreductase (PDB ID: 3HB5), crystal structure of *Escherichia coli* (PDB ID: 3T88) were used in this study. Molecular docking studies were performed using MOE 2008 software [16] in order to find out the possible binding modes of the most active compounds against the above receptors. It is an interactive molecular graphics program for calculating and displaying feasible docking modes of a receptor and ligand and complex molecules. It necessitates the ligand and the receptor as input in PDB format. The amino acid chain was kept and the water molecules and co-crystallized ligands were removed. The structure of complexes in PDB file format was created by Gaussian03 software. Crystal structure of different proteins were downloaded from the protein data bank (http://www.rcsb.org./pdb).

Results and Discussion

Characterization of Schiff base ligand (H_2L)

A novel brown symmetrical Schiff base ligand (H_2L), 4,4'-((1Z,1'Z)-(naphthalene-1,8-diylbis(azanylylidene))bis(methanylylidene)) dibenzaldehyde was prepared from 1,8-diaminonaphthalene and phthalaldehydic acid in a molar ratio of 1:2. The isolated Schiff base is stable at room temperature and soluble in most organic solvents. The elemental compositions (C, H and N) of the H_2L ligand is in good agreement with the calculated values based on proposed molecular formula. The infrared (IR) spectrum has an important role for identifying the functional groups and showing significant evidence for the interaction between the starting materials to get the Schiff base ligand (H_2L) [17].

The IR spectrum of the free Schiff base ligand was recorded in the range 400–4000 cm^{-1} showed peaks at 3429, 1610, 1593 and 1432 cm-^{1} which assigned to ν(OH) of carboxylic group, ν(C=N) azomethine group, $\nu(COO)_{asym}$ and $\nu(COO)_{sym}$ **,** respectively. The presence of this azomethine group suggested that the condensation process has been occurred and the Schiff base was formed [17]. Also, sharp band was appeared at 3429 cm^{-1} which corresponding to ν(OH) stretching vibration. The ^{1}H NMR spectrum of H_2L in DMSO-d_6 exhibited signals at 10.11 (s, 2H, carboxylic group), 8.05 (m, 2H, CH group) and 7.00-7.55 (m, 14H, aromatic ring). Also, the amino protons disappeared in the ^{1}H NMR spectrum which indicated the formation of azomethine group. The mass spectrum of the synthesized Schiff base ligand (H_2L) was recorded and the obtained molecular ion (m/z) peak at 424 amu confirmed the proposed formula in which the ligand moiety was $C_{26}H_{18}N_2O_4$ with atomic mass 422 g/mol. Also, the mass spectrum displayed multiple peaks corresponding to successive degradation of the ligand.

Characterization of metal complexes

Bidentate Schiff base ligand (H_2L) was synthesized and its complexes with some transition metal ions, Cr(III), Mn(II), Fe(III), Co(II), Ni(II), Cu(II), Zn(II) and Cd(II), were prepared. These prepared compounds were characterized by using elemental analysis (C, H, N and metal content), IR, ^{1}H NMR, molar conductance, UV-Vis, mass, SEM and thermal analyses (TG and DTG).

Elemental analysis

The elemental analyses results are summarized in experimental part. These results as well as the obtained mass spectra are in good agreement with the proposed formula. The complexes have verity in colors, stable in air and soluble in different solvents like DMF and DMSO and insoluble in ethanol, methanol and water. The results of elemental analyses suggested the formulae $[M(H_2L)Cl(H_2O)_3].Cl_2.2H_2O$ (M = Cr(III) and Fe(III)), $[M(H_2L)Cl(H_2O)_3]Cl.H_2O$ (M = Co(II), Ni(II), Cu(II), Mn(II) and $[M(H_2L)Cl_2(H_2O)_2].2H_2O$ (M = Zn(II) and Cd(II)). Based on the elemental analyses, all complexes were of stoichiometric ratio 1:1 and of MH_2L type.

Molar conductivity measurements

By using the relation (Λ_m = K/C), the molar conductance of the complexes (Λ_m) can calculated, where C is the molar concentration of the metal complex solutions. The chelates were dissolved in DMF and the molar conductivities of 10^{-3} M solutions at 25 °C were measured using the recommended procedure (Table 1). It is concluded from the results that the molar conductance values fall in the range 13–112 $\Omega^{-1}mol^{-1}cm^2$ indicative of their electrolytic nature for all complexes expect Zn(II) and Cd(II) complexes were non electrolytes [18,19].

IR spectra

IR spectrum of the H_2L ligand exhibited a broad band at 3429 cm^{-1} for ν(OH) of the carboxylic group. This band shifted in the spectra of the metal complexes to 3412–3436 cm^{-1}. Also, this may be due to presence of coordinated water in all complexes. For ν(C=N) stretching of the azomethine group, characteristic band of the Schiff base ligand in the spectrum of

H_2L ligand appeared at 1610 cm^{-1}, but in the spectra of the complexes appeared in the range of 1619–1635 cm^{-1}. This was attributed to the nitrogen atom of the (C=N) group coordinated to the metal ions [20–22]. Also, another medium band appeared at 1593 cm^{-1} was assigned to $(COO)_{asym}$ stretching in the free H_2L ligand that still approximately at the same band position in the complexes due to intramolecular hydrogen bonding. New bands appeared in the spectra of metal chelates at 909–923 and 819–835 cm^{-1} could be assigned to H_2O stretching of coordinated water [20-24]. Another new band appeared at 531–581 cm^{-1} which attributed to M–O stretching of coordinated water [20-24]. M–N stretching bands appeared at 447–482 cm^{-1} [20–22]. Thus, IR data showed that the Schiff base ligand was coordinated to the metal ions through the two N atoms of azomethine group in neutral bidentate manner.

^1H NMR spectra

The Schiff base ligand (H_2L) and its Zn(II) and Cd(II) complexes were also supported by the ^1H NMR spectral study. These spectra were recorded in DMSO-d_6. The ^1H NMR spectrum of the H_2L Schiff base ligand displayed three significant peaks at 10.11, 8.08 and 7.00–7.55 ppm with an integration equivalent to the hydrogen protons corresponding to the (s, 2H, carboxylic proton), (s, 2H, CH proton) and (m, 7H, aromatic rings), respectively [23, 24]. The ^1H NMR spectrum of the ligand showed singlet signals at 8.08 ppm which assigned to the CH protons. This signal still appeared in Zn(II) and Cd(II) complexes at the same postion. Other singlet signal with the integration corresponding to 2H at 10.11 ppm appeared at Schiff base ligand spectrum was assigned to the carboxylic protons. This peak appeared at approximately the same position in Zn(II) and Cd(II) complexes indicating its non involvement in coordination to metal ions. Also, the multiple signals within the range 7.00–7.55 ppm which assigned to the aromatic protons in the free ligand still appeared with shift in both Zn(II) and Cd(II) complexes within the range 7.10-7.50 ppm [25].

Scanning electron microscope (SEM)

The morphology, size and structure of the nanomaterials were conducted using field emission scanning electron microscope (SEM) [26]. The SEM micrographs of the Schiff base ligand (H_2L) and its $[Cd(H_2L)(H_2O)_2Cl_2].2H_2O$ complex were presented in (Figure 1). SEM images showed that the particles were agglomerated with controlled morphological structure [27]. It was evident from the SEM study that in the synthesized Cd(II) complex, crystals were found to grow up from just a single molecule to several molecules in an aggregate distribution with particle sizes that present in nanometers structures. As well, different characteristic shape of Cd(II) complex was identified and this SEM image was quite different from that of the Schiff base. The difference in the shape of the Schiff base metal complex was mainly dependent on the presence of metal ion.

The micrograph of the ligand indicated collected clouds shaped particles. The Cd(II) complex showed non-uniform clusters structure. The average particle size of the ligand was 20 nm, but the average particle size of the $[Cd(H_2L)Cl_2(H_2O)_2].2H_2O$ complex was 10-25 nm. The synthesized nanoparticle sized complex may help strongly in different fields including biological and industrial applications [28].

Electronic spectra of the Schiff base ligand and its metal complexes

The electronic spectra of the free H_2L ligand and its metal complexes were recorded in DMF solution with 10^{-4} mol L^{-1} concentration at room temperature. The absorption spectrum of the Schiff base ligand (H_2L) showed three absorption bands at 280, 340 and 442 nm. The first high intensity band was appeared at λ_{max} = 280 nm may be attributed to the π-π* transition of the aromatic rings. The second and third absorption bands that were showed at λ_{max} = 340 and 442 nm attributed to the n-π* transition of the azomethine group (C=N) and charge transfer, respectively [29-32]. Electronic spectra of the complexes showed bands which were shifted from the free ligand to 277-282 nm for π-π* and 338-342 nm for n-π* of aromatic rings and azomethine transitions, respectively, confirming the coordination of the azomethine nitrogen to the metal ions. These can be related to the binding of these coordination centers to the central metal ions. Also, bands appeared at 442- 451 nm in Cr(III), Fe(III), Ni(II), Cu(II) and Zn(II) complexes corresponding to charge transfer. Furthermore, three absorption bands in the visible region of Mn(II), Co(II) and Cd(II) complexes were observed at 602, 605 and 649 nm. These bands were considered to arise from the d-d splitting, which was generally too weak [33].

TABLE 1. Thermoanalytical results (TG and DTG) of H_2L and its metal complexes

Complex	TG range (^0C)	DTG_{max} (^0C)	n*	Mass loss Estim (Calcd) %	Total mass loss	Assignment	Residues
H_2L	34-228	102, 190	2	15.36 (15.21)		-Loss of C_4H_6N.	
	228-363	330	1	44.42 (44.81)		-Loss of $C_{10}H_6O_4$.	.....
	363-714	396	1	40.12 (40.20)	99.95 (100)	-Loss of $C_{13}H_6N$.	
$[Cr(H_2L)(H_2O)_3Cl]Cl_2.2H_2O$	15-113	74	1	6.32 (5.69)		-Loss of $2H_2O$.	$^1/_2Cr_2O_3$
	113-237	216	1	17.98 (19.68)		-Loss of Cl_2 and $3H_2O$.	
	237-536	289, 367	2	39.03 (40.56)		-Loss of $C_{15}H_{10}ClO_2$.	+9C
	536-1000	550, 857	2	12.53 (11.10)	75.86 (76.53)	$_{5^-}$.-Loss of $C_2H_8N_2O$ ·	
$[Mn(H_2L)(H_2O)_3Cl]Cl.H_2O$	12-92	68	1	7.21 (8.62)		-Loss of $^1/_2Cl_2$ and H_2O.	
	92-339	294	1	32.87 (31.93)		-Loss of $^1/_2Cl_2$, $3H_2O$,$C_6H_4N_2$.	MnO
	339-449	407	1	9.76 (9.35)		-Loss of C_3H_6O.	+3C
	449-1000	567	1	37.73 (38.70)	87.49 (88.65)	-Loss of $C_{16}H_{16}O_2$.	
$[Fe(H_2L)(H_2O)_3Cl]Cl_2.2H_2O$	33- 231	97, 198	2	11.32 (10.60)		-Loss of $^1/_2Cl_2$ and $2H_2O$.	
	231- 308	242	1	8.22 (8.09)		-Loss of $3H_2O$.	$^1/_2Fe_2O_3$
	308- 622	313	1	22.97 (22.19)		-Loss of Cl_2 and $C_3H_6N_2O_{0.5}$.	+4C
	622-1000	625	1	41.07 (40.35)	82.59 (81.23)	-Loss of $C_{19}H_{12}O_2$.	
$[Co(H_2L)(H_2O)_3Cl]Cl.H_2O$	11-218	67, 178	2	19.28 (20.03)		-Loss of Cl_2 and $3H_2O$.	
	218-323	270	1	7.81 (7.05)		-Loss of H_2O and HCN.	CoO+3C
	323-694	370,561	2	21.05 (21.61)		-Loss of $C_7H_4NO_2$.	
	694-1000	730	1	33.44 (33.48)	81.58 (82.18)	-Loss of $C_{15}H_{13}O$.	
$[Ni(H_2L)(H_2O)_3Cl]Cl.H_2O$	43-219	87, 205	2	19.27 (20.03)		-Loss of Cl_2 and $3H_2O$.	
	219-308	284	1	17.03 (17.94)		-Loss of H_2O, $C_6H_6N_2$.	NiO+C
	308-584	342, 425	2	30.12 (29.16)		-Loss of $C_{12}H_6O_2$.	
	584-1000	877	1	22.49 (22.75)	88.91 (89.88)	-Loss of $C_{10}H_6O$.	
$[Cu(H_2L)(H_2O)_3Cl]Cl.H_2O$	27-156	107	1	9.67 (10.92)		-Loss of $^1/_2Cl_2$ and $2H_2O$.	
	156-252	206	1	13.34 (14.20)		-Loss of $^1/_2Cl_2$ and $3H_2O$.	CuO+7C
	252-389	329	1	23.11 (23.17)		-Loss of $C_9H_{10}N_2$.	
	389-1000	836	1	26.48 (27.93)	72.48 (75.84)	-Loss of $C_{10}H_8O_3$.	
$[Zn(H_2L)(H_2O)_2Cl_2]2H_2O$	14-216	71, 161	2	10.71 (11.42)		-Loss of $4H_2O$.	
	216-434	361	1	27.21 (28.32)		-Loss of Cl_2 and $C_6H_8N_2$	ZnO+C
	434-1000	512,950	2	39.65 (39.21)	77.56 (78.95)	-Loss of $C_{16}H_{10}O_3$.	
$[Cd(H_2L)(H_2O)_2Cl_2]2H2O$	41-202	96	1	6.46 (6.28)		-Loss of $2H_2O$.	
	202-485	238,321	2	51.03 (52.28)		-Loss of $2H_2O$, Cl_2 and $C_{14}H_{10}N_2O_2$.	CdO
	485-1000	610-846	2	24.77 (25.45)	82.26 (83.02)	-Loss of $C_{12}H_8O$.	

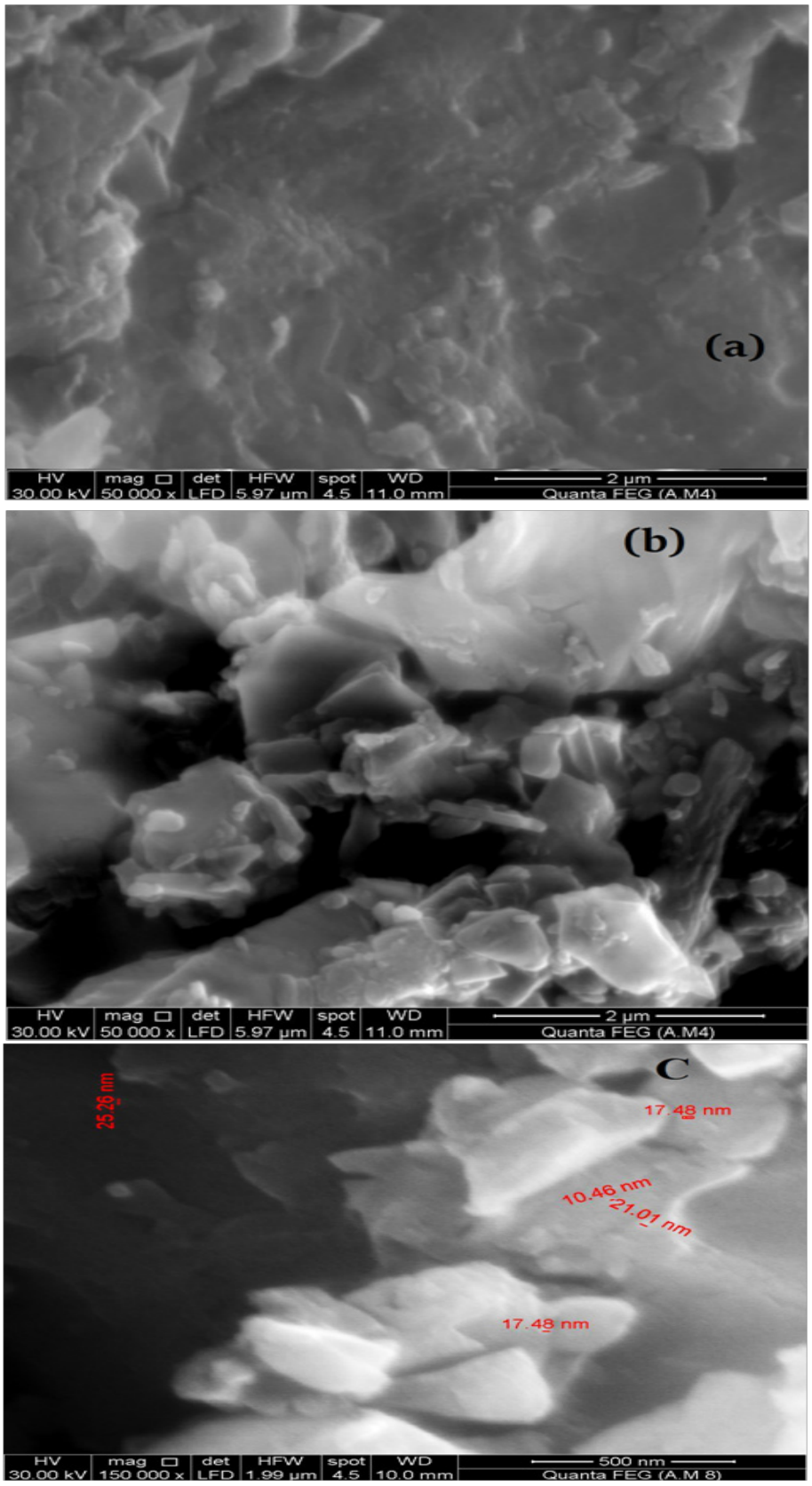

Fig. 1. The SEM images of the nanoparticles produced a) Schiffbase ligand (H2L) and b) and c) SEM images with different magnifications of[Cd(H2L)(H2O)2Cl2]2H2O complex.

The electronic spectrum of Cr(III) complex showed three spin allowed bands at 18150, 24010 and 26150 cm^{-1}. These bands may be assigned to $^4A_{2g}(F) \rightarrow {}^4T_{2g}(F)$, $^4A_{2g}(F) \rightarrow {}^4T_{1g}(F)$ and $^4A_{2g}(F) \rightarrow {}^4T_{1g}(P)$ transitions indicating the octahedral geometry of the complex. The magnetic moment was found to be 4.15 B.M. which confirmed octahedral geometry of Cr(III) complex [21].

The Mn(II) complex showed three spin allowed bands at 17280, 21130 and 25950 cm^{-1}. These bands may be assigned to $^4T_{1g} \rightarrow {}^6A_{1g}$, $^4T_{2g}(G) \rightarrow {}^6A_{1g}$ and $^4T_{1g}(D) \rightarrow {}^6A_{1g}$ transitions indicating the octahedral geometry of the complex. The magnetic moment was 5.13 B.M. which confirmed octahedral geometry of Mn(II) complex [6].[6]

The Fe(III) complex showed three spin allowed bands at 22460, 20190 and 16565 cm^{-1}. These bands may be assigned to $^4T_{2g}(G) \rightarrow {}^6A_{1g}$, $^4T_{2g}(G) \rightarrow {}^6A_{1g}$ and $^4T_{1g}(D) \rightarrow {}^6A_{1g}$ transitions indicating the octahedral geometry of the complex. The magnetic moment was 5.02 B.M. which confirmed octahedral geometry of Fe(III) complex.

The Co(II) complex showed three spin allowed bands at 22950, 20110 and 16245 cm^{-1}. These bands may be assigned to $^4T_{1g}(F) \rightarrow {}^4T_{2g}(F)$, $^4T_{1g}(F) \rightarrow {}^4A_{2g}(F)$ and $^4T_{1g}(F) \rightarrow {}^4T_{2g}(P)$ transitions indicating the octahedral geometry of the complex. The magnetic moment was 4.87 B.M. which confirmed an octahedral geometry of Co(II) complex [34].

The Ni(II) complex showed three spin allowed bands at 28100, 22185 and 11970 cm^{-1}. These bands may be assigned to $^3A_{2g} \rightarrow {}^3T_{1g}(P)$, $^3T_{1g}(P) \rightarrow {}^3A_{2g}$ and $^3A_{2g}(F) \rightarrow {}^3T_{1g}(F)$ transitions indicating the octahedral geometry of the complex. The magnetic moment was 3.98 B.M. which confirmed octahedral geometry of Ni(II) complex [21, 22].

The Cu(II) complex showed three spin allowed bands at 21016, 17258 and 14181 cm^{-1}. These bands may be assigned to $^2B_{1g} \rightarrow {}^2A_{1g}$, $^2B_{1g} \rightarrow {}^2E_g$ and $^2B_{1g} \rightarrow {}^2B_{2g}$ transitions indicating the octahedral geometry of the complex. The magnetic moment was 1.89 B.M. which confirmed octahedral geometry of Cu(II) complex [34]

The Zn(II) and Cd(II) complexes were diamagnetic. According to the empirical formulae, an octahedral geometry for the Zn(II) and Cd(II) complexes was suggested.

Thermal analysis of Schiff base ligand and its metal complexes

Thermal properties of the H_2L ligand and its metal complexes were investigated with TG/DTG under the ambient temperature up to 1000 °C. The thermal analysis data are summarized in Table 1. All of the complexes gave different curves containing different decomposition steps. The experimental weight loss values for the complexes were in good agreement with the calculated values [35]. The thermal decomposition process of the free H_2L Schiff ligand involved three decomposition steps. Decomposition of the H_2L ligand started at 34 °C and finished at 1000 °C. The first stage corresponded to two steps of decomposition involved the removal of one molecules of C_4H_6N in the 34–228 °C range, and was accompanied by a weight loss of 15.36% (calcd 15.21%). The second stage decomposition occurred in the 228–363°C range, corresponding to the loss of $C_{10}H_6O_4$ molecule and was accompanied by a weight loss of 35.65% (calcd 35.39%). The final step of decomposition occurred in the 363 – 1000 °C range, corresponding to the loss of $C_{13}H_6N$ molecule and was accompanied by a weight loss of 40.12% (calcd 40.20%).

The TG curve of $[Cr(H_2L)Cl(H_2O)_2]Cl_2.2H_2O$ complex showed six decomposition steps within the temperature range of 30–1000 °C. The first decomposition step was accompanied by loss of two water molecules in the temperature range of 30–113 °C with an estimated mass loss of 5.32% (calcd. 5.69%). The second stage of decomposition showed loss of three water molecules and chlorine gas at 113–237 °C with an estimated mass loss of 19.98% (calcd. 19.68%). The third and fourth steps of decomposition showed loss of $C_{15}H_{10}ClO_2$ at 237–536 °C with an estimated mass loss of 39.03% (calcd. 40.56%).The last two steps of decomposition showed loss of $C_2H_8N_2O_{0.5}$ molecule at 536–1000 °C with an estimated mass loss of 11.53% (calcd. 11.10%). Thereafter, the percentage of the residue corresponds to chromium oxide contaminated with carbon. The total estimated mass loss was found to be 75.86% (calcd. 76.53%).

TG curve of the $[Mn(H_2L)Cl(H_2O)_3]Cl.2H_2O$ complex showed four steps of decomposition. The first stage of decomposition occurred in the 25–92 °C temperature range, corresponding to the loss of water molecule and half of chlorine gas, and was accompanied by a mass loss of 7.21% (calcd. 8.62%). The second and third stages of

decomposition involved the removal of three water molecules, $C_9H_{10}N_2O$ and half of cholrine gas at 92–449 °C temperature range and were accompanied by mass loss of 42.63% (calcd. 41.28%). The fourth stage of decomposition involved the removal of $C_6H_{16}O_2$ molecule at 449-1000 °C temperature range and was accompanied by mass loss of 37.73% (calcd. 38.70%). The total mass loss amounted to 87.49% (calcd. 88.65%), and manganese oxide contaminated with carbon was remained as a residue.

The $[Fe(H_2L)Cl(H_2O)_3]Cl_2.2H_2O$ chelate exhibited five decomposition steps. The first and second steps occurred in the temperature range of 32–231 °C. These steps assigned to loss of two water molecules and half of chlorine gas with estimated mass loss of 11.32% (calcd. = 10.60%). The third stage of decomposition involved the removal of three water molecules at 231- 308 °C temperature range and was accompanied by mass loss of 8.22% (calcd. 8.09%). The fourth stage of decomposition involved the removal of chlorine gas and $C_3H_6N_2O_{0.5}$ at 308- 622 °C temperature range and was accompanied by mass loss of 22.97% (calcd. 22.19%). The last stage of decomposition involved the removal of $C_{19}H_{12}O_2$ at 622-1000 °C temperature range and was accompanied by mass loss of 41.07% (calcd. 40.35%). The overall mass loss amounted to 82.59% (calcd. = 81.23%) leaving 1/2 Fe_2O_3 and contaminated carbon as the residue of decomposition.

The $[Co(H_2L)(H_2O)_3Cl]Cl.H_2O$ complex lost upon heating $5H_2O$ and Cl_2 in the first and second decomposition within the temperature range of 30–218 °C, at maximum peaks temperatures 67 and 178 °C with estimated mass loss of 19.28% (calculated mass loss = 20.03%). The third step accounted for the loss of water molecule and HCN molecule within the temperature range of 218–323 °C, at maximum peak temperature 270 °C, with estimated mass loss of 7.81% (calculated mass loss = 7.05%). The last three steps accounted for the loss of $C_7H_5NO_2$ and $C_{15}H_{12}O$ fragments within the temperature range of 323–1000 °C, at maximum peak temperature 370, 561 and 730 °C, with estimated mass loss of 54.49% (calculated mass loss = 55.09% leaving CoO contaminated with carbon as residue of decomposition. The overall weight loss amounted to 81.58% (calculated mass loss = 82.18%).

The Ni(II) complex gave decomposition pattern started at 43 °C and finished at 1000 °C with four stages. The first stage was two steps within the temperature range of 43–219 °C with maximum peak temperature at 87 and 205 °C and represented the loss of three hydrated water molecules and Cl_2 with a found mass loss of 19.27% (calculated mass loss = 20.03%). The second stage was one step and represented the loss of H_2O and $C_4H_6N_2$ molecules with a mass loss of 17.03% (calculated mass loss = 17.94%) within the temperature range 219–308 °C and maxima peak temperature at 284 °C. The third stage was two steps representing the loss of $C_{12}H_6O_2$ molecule with a mass loss of 30.12% (calculated mass loss = 29.16%) within the temperature range 308–584 °C. The final stage was one step representing the loss of $C_{10}H_6O$ molecule with a mass loss of 22.49% (calculated mass loss =22.73%) within the temperature range 584–1000 °C. At the end of the thermogram, the metal oxide NiO with carbon were the residues, which was in good agreement with the calculated metal content obtained and the results of elemental analyses. The overall weight loss amounted to 88.91% (calculated mass loss = 89.88%).

The TG curve of the Cu(II) complex showed that the first and the second decomposition steps correspond to mass loss 25.01% (calculated mass loss = 25.12%) which occurred within the temperature range from 27 to 156 °C with maximum peaks temperatures at 107 and 206 °C and represented the loss of Cl_2 and $5H_2O$ molecules. The third step within the temperature range 252–389 °C with maximum peak temperature at 328 °C may be attributed to the decomposition of $C_9H_{10}N_2$ molecule with found mass loss of 23.11% (calculated mass loss = 23.17%). The final step started at 389°C and ended at 1000°C with maximum peak temperature at 836 °C and may be accounted to the loss of $C_{10}H_8O_3$ molecule with mass loss of 26.48% (calculated mass loss = 27.93%), leaving behind CuO contaminated with carbon as residues of decomposition. The overall weight loss amounted to 74.48% (calculated mass loss = 75.84%).

For Zn(II) complex, the first stage included two steps of decomposition correspond to mass loss of 10.71% (calculated mass loss = 11.42%) within the temperature range 14-216 °C with maximum peak temperature at 71 and 161 °C and represented the loss of four hydrated water molecules. The second step within the temperature range 216–434°C with maximum peak temperature at 361 °C may be attributed to the decomposition of Cl_2 and $C_6H_8N_2$ molecules with found mass loss of 28.21% (calculated mass loss = 28.32%). The final stage containing two steps started at 434 °C and ended

at 1000 °C with maximum peak temperature at 512 and 950 °C and may be accounted to the loss of $C_{16}H_{10}O_3$ molecule with mass loss of 39.65% (calculated mass loss = 39.21%), leaving behind ZnO and contaminated with carbon as residues of decomposition. The overall weight loss amounted to 78.56% (calculated mass loss = 78.95%).

TG curve of the $[Cd(H_2L)(H_2O)_2Cl_2].2H2O$ complex showed five steps of decomposition. The first step of decomposition occurred in the temperature range of 41–202 °C and is associated with the loss of two hydrated water with an estimated weight loss of 6.46% (calcd. 6.28%). The second and third steps of decomposition occurred in the temperature range of 202–485°C and are associated with the loss of $2H_2O$, Cl_2 and $C_{14}H_{10}N_2O_2$ molecules and with an estimated weight loss of 51.03% (calcd. 52.28%). The final stage including two steps of decomposition occurred in the temperature range of 485–1000 °C and was associated with the loss of $C_{12}H_8O$ molecule and with an estimated weight loss of 24.77% (calcd. 25.45%). Thereafter the weight of the residue corresponds to cadmium oxide with total weight loss percentage of 82.26% (calcd. 83.02%).

Structural Interpretation

The structures of Schiff base ligand (H_2L) and its metal complexes were characterized using various physico-chemical and spectral data. Accordingly, the structures of the complexes have been confirmed and the proposed structural formulas of the complexes were shown in Fig.2.

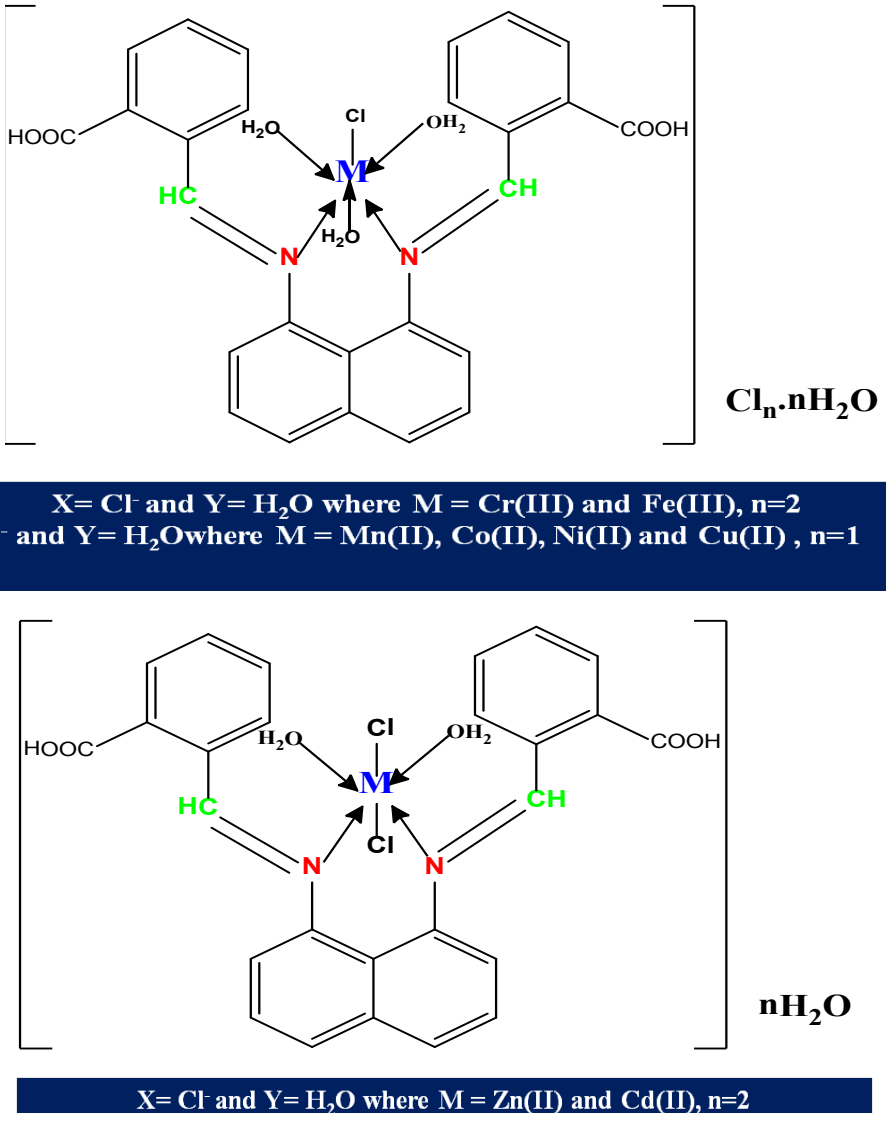

Fig. 2. The proposed structures of Schiff base metalcomplexes.

Biological Activity

Anti-microbial activity

It is well known that metal complexes have higher antibacterial activity than the associated free Schiff base ligand which can be attributed to the chelation of the Schiff base with metal ions as metal chelates displaying both polar and non-polar properties. This makes them suitable for penetration into cells and tissues. The polarity of the metal ion will be decreased to a greater extent because of the overlap of the ligand orbital upon complexation, and partial sharing of the positive charge of the metal ion with donor groups. Chelation enhances the delocalization of π-electrons over the whole chelating ring and induces the penetration of complexes into lipid membranes. It also increases the lipophilic and hydrophilic nature of the central metal ions contributing to liposolubility and permeability through the lipid layer of cell membranes. Furthermore, lipophilicity, which is responsible for the rate of entry of molecules into cells, is improved by coordination, so a metal complex can become more active than the free Schiff base ligand.

The newly synthesized Schiff base ligand (H_2L) and its metal complexes were screened for their antifungal and antibacterial activities. The tested compounds showed variable antibacterial activity against both Gram(+) bacteria: [*Streptococcus mutans*, *Staphylococcus aureus*], Gram(−) bacteria: [*Escherichia coli* and *Pseudomonas aeruginosa*] and fungal species such as *Candida albicans* and *Aspergillus fumigates*. The efficiencies of the Schiff base ligand (H_2L) and its complexes have been tested against these organisms (Gram(+ve), Gram (−ve) and fungi) were shown in supplementary Fig. 3). Also, these activities were listed in Table 2. The metal complexes exhibited higher inhibition against all microorganisms tested compared with free H_2L ligand [36]. The biological activity of many ligands increased after the coordination with metal ions.

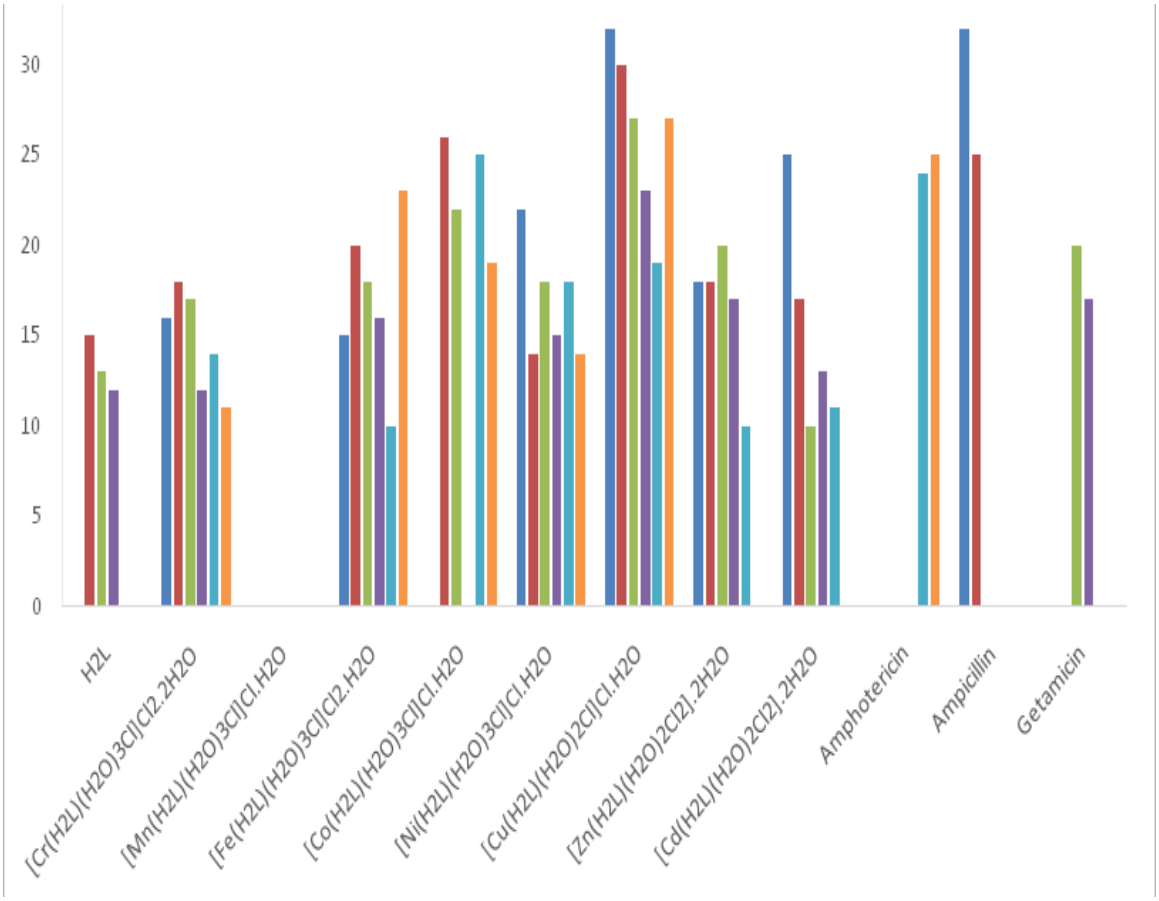

Fig. 3.Biological activity of H2Lligand and its metal complexes.

TABLE 2. Biological activity of Schiff base ligand (H_2L) and its metal complexes.

	Inhibition zone diameter (mm / mg sample)					
	(Gram positive)		*(Gram negative)*		*(fungus)*	
	Bacillus Subtilis	***Streptococcus pneumoniae***	***Escherichia coli***	***Pseudomonas aeruginosa***	***Aspergillus fumigates***	***Candida albicans***
H_2L	0	15	13	12	0	0
$[Cr(H_2L)(H_2O)_3Cl]Cl_2.2H_2O$	16	18	17	12	14	11
$[Mn(H_2L)(H_2O)_3Cl]Cl.H_2O$	0	0	0	0	0	0
$[Fe(H_2L)(H_2O)_3Cl]Cl_2.2H_2O$	15	20	18	16	10	23
$[Co(H_2L)(H_2O)_3Cl]Cl.H_2O$	0	26	22	0	25	19
$[Ni(H_2L)(H_2O)_3Cl]Cl.H_2O$	22	14	18	15	18	14
$[Cu(H_2L)(H_2O)_2Cl]Cl.H_2O$	32	30	27	23	19	27
$[Zn(H_2L)(H_2O)_2Cl_2].2H_2O$	18	18	20	17	10	NA
$[Cd(H_2L)(H_2O)_2Cl_2].2H_2O$	25	17	10	13	11	NA
Amphotericin	**------**	**------**	**-----**	**------**	**24**	**25**
Ampicillin	**32**	**25**	**------**	**------**	**------**	**-----**
Getamycin	**------**	**------**	**20**	**17**	**------**	**------**

The H_2L–metal complexes of Mn(II), Cu(II) and Ni(II) showed specific antifungal activity of inhibition zone of diameter ranged from 13.0 to 29.0 mm. [37] All the complexes showed definite bacterial growth inhibition for the four organisms with inhibition zone diameter ranged from 10.0 to 32.0 mm. The results of antimicrobial activities are presented in Table 2. The H_2L ligand showed activity against the four bacterial organisms in the range of 10.0–17.0 mm [38]. The Cr(III), Mn(II) and Cu(II) complexes showed the best bacterial inhibition among all the complexes with inhibition zone diameter ranged from 12.0 to 32.0 mm indicating that the coordination of the H_2L ligand to these metal ions has enhanced its antimicrobial activity. The activities of the prepared Schiff base ligand and its metal complexes were confirmed by calculating the activity index according to the following relation [39,40]. The enhanced antimicrobial activity of all complexes against these organisms can be attributed to the concept of chelation. Because the positive charges of the metal were partially shared with the donor atoms found in the ligand and there was possible π-electron delocalization over the metal complex formed. The lipophilic character of the metal complex increases and supports its permeation more efficiently through the lipid layer of the micro-organisms. This permits easy binding and penetration of the complex in the cellular structure of the pathogens. The chelation leads to make the ligand act as more powerful and potent bactereostatic agents. This inhibits the growth of bacteria more than the parent ligand. It was suspected that factors such as conductivity, solubility, dipole moment and cell permeability mechanism may be influenced by the presence of metal ion. This might be the possible reason for increasing the activity after chelation [41,42]

ANTICANCER ACTIVITIES

In various human diseases, cancer considered as the most severe disease to which humans were subjected and yet no effective drugs or any methods of control are available to treat it. So, it is necessary to identify novel, selective, potent and

less toxic anticancer agents which became one of the most pressing problems. Cancer is a complex disease that is normally correlated to a wide range of escalating effects both at the cellular and molecular levels [43]. The cytotoxic ability of Schiff base ligand and its metal complexes were evaluated against breast carcinoma cells (MCF-7 cell line), which is one of the most common form of cancer. So firstly, all the synthesized complexes screened against single dose experiment on MCF-7 cell line with concentration 100 µg/ml. The in vitro screening of the compounds showed that inhibition ratio for ligand is about 75 % and its metal complexes were found to be with inhibition ratio values between 40 and 79 %. The highest inhibition ratio value (79%) corresponding to Cd(II) complex. Also the relationship between tested compound concentration and cell viability was plotted to calculate IC_{50} (µg/ml) (the value which corresponds to the concentration required for 50% inhibition cell viability) [44]. Furthermore, four concentrations (0, 12.5, 25 and 50 µg/ml) and the IC_{50} values of more active complexes with inhibition ratio value >70% were measured and listed in Table 3 and supplementary Fig. 4. These active compounds were screened against single dose experiment on human normal melanocytes (HFB-4) cell line with concentration 100 µg/ml and proved to be low toxic to them (surviving fraction is 85 %). The ligand showed IC_{50} value of 20.5 µg/mL towards human breast cancer cell lines (MCF-7) and that for some selected complexes (Cr(III), Mn(II), Cu(II) and Cd(II)) was in the range of 17 – 38 µg/mL. While the Fe(III) complex did not show any IC_{50} value. It was clear from Table 3 that Cd(II) complex had very high cytotoxic activity against MCF-7 cell line (its IC_{50} value = 17.6 µg/mL).

From these data, it is confirmed that Cd(II) complex has an outstanding IC_{50} value of 17.6 µg ml^{-1} and a very low concentration of this complex can be used to produce 50% inhibition of cell growth [45, 46].

TABLE 3.Antibreastic cancer activity of Schiff base ligand (H_2L) and itsmetal complexes

Complex	Concn. (mg/mL)	Surviving fraction (MCF-7) 0.0	5.0	12.5	25.0	50.0	IC_{50} (mg/mL)
H_2L		1.0	0.848	0.670	0.426	0.272	20.5
$[Cr(H_2L)(H_2O)_3Cl]Cl_2.2H_2O$		1.0	0.838	0.663	0.530	0.295	28.3
$[Mn(H_2L)(H_2O)_3Cl]Cl.H_2O$		1.0	0.850	0.728	0.654	0.344	37.6
$[Co(H_2L)(H_2O)_3Cl]Cl.H_2O$		1.0	0.811	0.689	0.480	0.229	21.0
$[Cu(H_2L)(H_2O)_3Cl]Cl.H_2O$		1.0	0.924	0.850	0.543	0.261	22.6
$[Cd(H_2L)(H_2O)_2Cl_2]2H_2O$		1.0	0.749	0.639	0.310	0.235	17.6

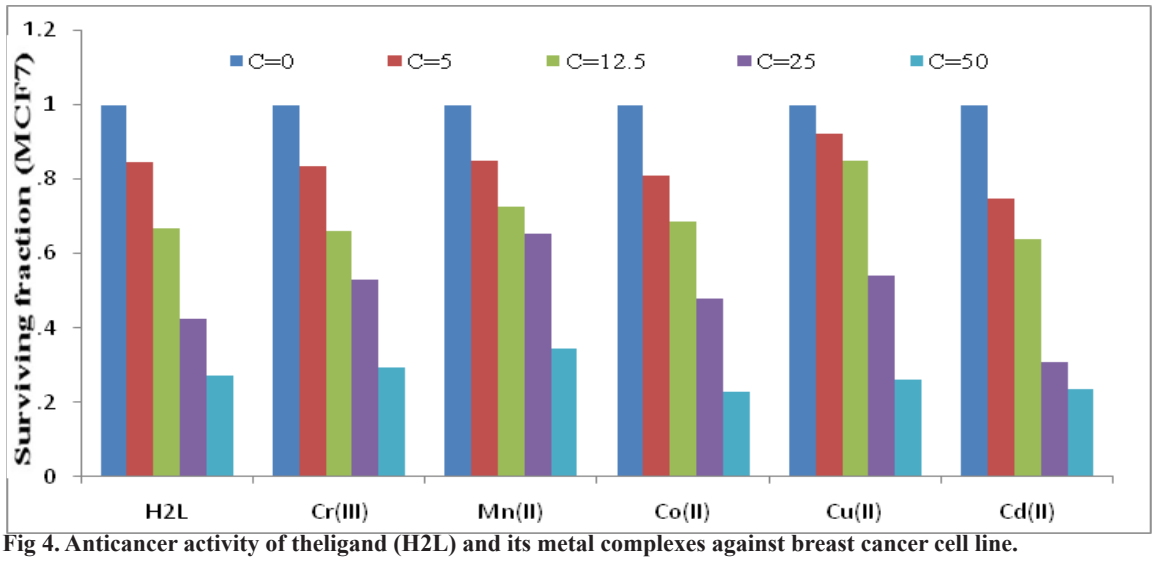

Fig 4. Anticancer activity of theligand (H2L) and its metal complexes against breast cancer cell line.

Molecular Docking

Targeting the minor groove of DNA through binding to a small molecule has long been considered an important tool in molecular recognition of a specific DNA-sequence. DNA is considered a major biological target for metal complexes that had pharmacological activity. In this context, molecular docking between H_2L with four possible biological targets: receptors of crystal structure of *S. aureus* (PDB ID: 3Q8U), crystal structure of sialidase NanC of *Streptococcus pneumoniae* (PDB ID: 4YW4), receptors of breast cancer mutant oxidoreductase (PDB ID: 3HB5), crystal structure of *Escherichia coli* (PDB ID: 3T88) were performed. The structures of these macro molecules were obtained from the Protein Data Bank. The calculated binding energies for the interaction with these proteins were listed in Tables 4. The 3D plot curves of docking with free H_2L were shown in Figure 5.

From these data it concluded the following notes:

1. First, the H_2L showed strong binding affinities for all proteins.
2. The binding energy for the interaction of H_2L with the receptor protein 3Q8U was about five times more than any other tested protein confirming the high activity of this compound against this protein receptor [47].
3. A closer look at the interactions indicated that the presence of hetero atoms like oxygen and nitrogen were critical to how the compound bind [48].
4. Generally speaking, H-acceptor interaction dominates the binding of the synthesized Schiff base to the different receptors.

Conclusions

In summary, the work reported involved the synthesis and spectroscopic characterization of series of Cr(III), Mn(II), Fe(III), Co(II), Ni(II), Cu(II), Zn(II) and Cd(II) complexes with a new Schiff base ligand prepared by condensation of 1,8-diaminonaphtalene with phthalaldehydic acid. The complexes were characterized using various physiochemical techniques. The Schiff base ligand acts as a bidentate (NN) ligand through the two azomethine nitrogen atoms and all complexes showed octahedral geometry. Their molar conductance values confirmed that Zn(II) and Cd(II) complexes are non-electrolytes, while the Mn(II), Co(II), Ni(II) and Cu(II) complexes are 1:1 electrolytes and the Cr(III) and Fe(III) complexes are 1:2 electrolytes. From elemental analysis, the complexes have composition of the MH_2L type with general formulae $[M(H_2L)(H_2O)_3Cl]Clx.nH_2O$ (M = Mn(II), Co(II), Ni(II) and Cu(II) x = n = 1; Cr(III) and Fe(III), x = n = 2), $[M(H_2L)(H_2O)_2Cl_2]nH_2O$ (M = Zn(II) and Cd(II) n = 2). The ligand and metal complexes are found to possess appreciable antibacterial activity, and the Cu(II) complex which also has highest activity. The Ni(II), Cu(II) and Cd(II) complexes have high antifungal activity. In addition, the cytotoxicity of the Cd(II) complex indicated a higher anticancer activity than the others with IC_{50} of 17.6 µg mL^{-1}, which might become a good anticancer agent in clinical trials or biological agents.

TABLE 4. Energy values obtained in docking calculations of H_2L with different protein receptors

Protein receptor	Ligandmoiety	Receptor	Interaction	Distance	E (kcal/mol)
3T88	O 44	N PHE 162 (A)	H-acceptor	2.94	-2.7
	O 48	OH TYR 97 (A)	H-acceptor	3.29	-0.8
	6-ring	N GLY 133 (A)	pi-H	3.89	-0.9
4YW4	O 49	ND1 HIS 314 (A)	H-donor	3.08	-2.3
	O 48	N PHE 316 (A)	H-acceptor	3.25	-3.1
	O 49	NH1 ARG 718 (A)	H-acceptor	3.03	-1.5
	6-ring	NH2 ARG 397 (A)	pi-cation	3.86	-0.6
	6-ring	NH2 ARG 397 (A)	pi-cation	4.45	-0.8
	O 49	ND1 HIS 314 (A)	H-donor	3.08	-2.3
	O 48	N PHE 316 (A)	H-acceptor	3.25	-3.1
	O 49	NH1 ARG 718 (A)	H-acceptor	3.03	-1.5
	6-ring	NH2 ARG 397 (A)	pi-cation	3.86	-0.6
3HB5	O 44	N GLY 94 (X)	H-acceptor	3.24	-2.5
	6-ring	NE ARG 37 (X)	pi-cation	4.12	-1.0
	6-ring	NH2 ARG 37 (X)	pi-cation	3.5	-0.7
	6-ring	6-ring PHE 192 (X)	pi-pi	3.98	0.0
3Q8U	O 49	ND1 HIS 115 (A)	H-donor	3.08	-3.1
	O 48	NZ LYS 9 (A)	H-acceptor	3.01	-11.3
	O 44	MG MG 159 (A)	metal	2.32	-1.8
	6-ring	CA SER 90 (A)	pi-H	4.53	-0.6
	6-ring	NH1 ARG 102 (A)	pi-cation	3.42	-0.6

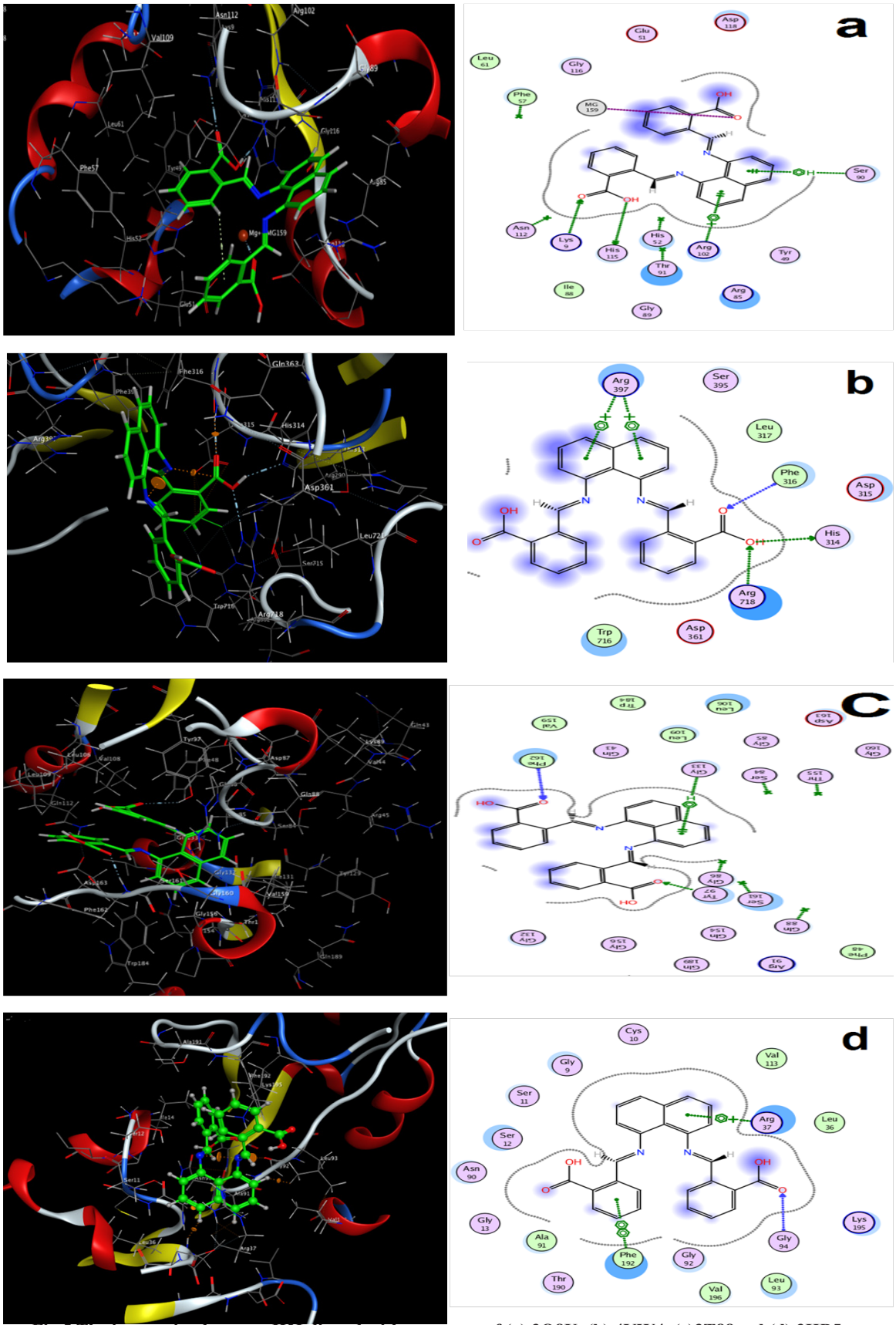

Fig.5 The interaction between H2L ligand with receptors of (a) 3Q8U, (b) 4YW4, (c)3T88and (d) 3HB5.

References

1. Z. Cimerman, S. Miljanic and N. Galic, Croatica Chemica Acta, 73 (1), 81- 95 (2000).
2. P. Singh, R. L. Goel and B. P. Singh, J. Indian Chem. Soc., , 52, 958 (1975).
3. B. F. Perry, A. E. Beezer, R. J. Miles, B. W. Smith, J. Miller and M. G. Nascimento, Microbois., , 45, 181 (1988).
4. A. Elmali, M. Kabak and Y. Elerman, J. Mol. Struct., , 477, 151 (2000).
5. P. R. Patel, B. T. Thaker and S. Zele, Indian J. Chem., , 38 A, 563 (1999).
6. M. Valcarcel and M. D. Laque de Castro, "Flow-Throgh Biochemical Sensors", Elsevier, , Amsterdam (1994).
7. U. Spichiger-Keller, "Chemical Sesors and Biosensors for Medical and Biological Applications", Wiley-VCH, Weinheim (1998).
8. J. F. Lawrence and R. W. Frei, "Chemical Derivatization in Chromatography", Elsevier, , Amsterdam (1976).
9. S. Patai, Ed., "The Chemistry of the Carbon-Nitrogen Double Bond", J. Wiley & Sons, , London (1970).
10. E. Jungreis and S. Thabet S, "Analytical Applications of Schiff bases", Marcell Dekker, , New York (1969).
11. Metzler C M, Cahill A and Metzler D E, J. Am. Chem. Soc., , 102, 6075 (1980).
12. G. O. Dudek and E. P. Dudek, Chem. Commun.,. 464 (1965).
13. A. Albert, Selective Toxicity: Physico-chemical Basis of Therapy (6th Edition), Wiley, New York (1979).
14. S. Chandra, D. Jain, A. K. Sharma, P. Sharma, Molecules,14, 174 (2009).
15. P. Skehan, R. Storeng, D. Scudiero, A. Monks, J. McMahon, D.Vistica, J. T. Warren, H. Bokesch, S. Kenney, M. R. Boyd, J. National Cancer Instit., 82, 1107 (1990).
16. Molecular Operating Environment (MOE.10), Chemical Computing Group Inc., Montreal, QC, Canada (2008).
17. N. M. Hosny, M. A. Husien, F. M. Radwan, N. Nawar, Mol. Str. , 1143, 176 (2017).
18. M. Hanif, Z. H. Chohan, Spectrochim. Acta A, 104, 468 (2013).
19. A. M. A. Alaghaz, H. A. Bayoumi, Y. A. Ammar, S. A. Aldhlmani, J. Mol. Struct. , 1035, 383 (2013).
20. W.H. Mahmoud, G.G. Mohamed, A.M. Refat, Appl. Organomet. Chem. 31(11) 1-19(2017).
21. W. H. Mahmoud, R.G. Deghadi, M. M.I. El Desssouky, G. G. Mohamed, Appl. Organometal. Chem, , article in press (2019).
22. WH Mahmoud, RG Deghadi, GG Mohamed. J Therm Anal Calorim. ;127(3):2149–71 (2017).
23. W.H. Mahmoud, G.G. Mohamed, O.Y. El-Sayed, appl. Organomet. Chem. 32(2) , 1-21 (2018).
24. W.H. Mahmoud, N.F. Mahmoud, G.G. Mohamed, Appl. Organomet. Chem. 31(12) 1-19 (2017).
25. A. A. Abdel Aziz, I. S. A. El-Sayed, M. M. H. Khalil, Appl. Organometal. Chem., In Press (2017).
26. Z. Parsaee, K. Mohammadi, Mol. Str. , 1137, 512 (2017).
27. N. K. Poonia, S. Siddiqui, M. D. Arshad, D. Kumar, Spectrochim. Acta A, 155, 146 (2016).
28. A. M. A. Alaghaz, M. E. Zayed, S. A. Alharbi, Mol. Str. ,1084, 36 (2015).
29. N. Mishra, K. Poonia, S. K. Soni, D. Kumar, Polyhedron,120, 60 (2016).
30. W. H. Mahmoud, N. F. Mahmoud, G. G. Mohamed, J. Coord.Chem. , 70:20, 3552-3574 (2017).
31. Z. Beigi, A. H. Kianfar, G. Mohammadnezhad, H. Görls, W.Plass, Polyhedron, 134, 65 (2017).
32. N. Ribeiro, S. Roy, N. Butenko, I. Cavaco, T. Pinheiro, I. Alho, F. Marques, F. Avecilla, J. C. Pessoa, I. Correia, J. Inorg.Biochem. , 174, 63 (2017).
33. Y. Liu, G. Lian, D. Yin, B. Su, Spectrochim. Acta A, 100, 131 (2013).
34. W.H. Mahmoud, M.A. Diab, A.Z. El-Sonbati, S.Y. Abbas, J of Molecular structure, 1181, 645-659 (2019),
35. E Adiguzel, F Yilmaz, M Emirik, M Ozil. J Mol Struct. ;1127:403–12 (2017).
36. W. H. Mahmoud, N. F. Mahmoud, G. G. Mohamed, A. Z.El-Sonbati, A. A. El-Bindary, J.

Mol. Struct., 1095, 15 (2015).

37. H. W. Rossmore, in Disinfection, Sterilization and Preservation, fourth ed. (Ed: S. S. Block), Lea and Febinger, Philadelphia, 290 (1991).

38. A. D. Russell, in Disinfection, Sterilization and Preservation, fourth ed. (Ed: S. S. Block), Lea and Febinger, Philadelphia, 27 (1991).

39. I. Muhammad, I. Javed, I. Shahid, I. Nazia, Turk. J. Biol., 31, 67 (2007).

40. T. D. Thangadurai, K. Natarajan, Indian J. Chem. A, 40, 573 (2001).

41. Z. H. Chohan, M. Praveen, Appl. Organometal. Chem. , 15, 617 (2001).

42. Z. H. Chohan, C. T. Supran, A. Scozzafava, J. Enz. Inhib. Med. Chem. , 19, 79 (2004).

43. S. J. Kirubavathy, R. Velmurugan, R. Karvembu, N. S. P.Bhuvanesh, I. V. M. V. Enoch, P. M. Selvakumar, D. Premnath, S. Chitra, Mol. Str. , 1127, 345 (2017).

44. C. M. Sharaby, M. F. Amine, A. A. Hamed, Mol. Str. , 1134, 208 (2017).

45. L. H. Abdel-Rahman, A. M. Abu-Dief, N. A. Hashem, A. A. Seleem, Int. J. Nano Chem., 1, 79 (2015).

46. Nadia G. Zaki1, Walaa H. Mahmoud, Ahmed M. El Kerdawy, Abanoub Abdallah , Gehad G. Mohamed, Accepted Manuscript, Egyptian journal of chemistry, (2019).

47. F.A. Beckford, A. Brock, A. Gonzalez-Sarrnas, N.P. Seeram. J. Mol. Str. 1121, 156 (2016).

48. K. Zheng, M. Yan, Y. Li , Z. Wu, C. Yan. Eur. J. Med. Chem., 109, 47 (2016).